J Nanostruct 16(1): 595-602, Winter 2026

RESEARCH PAPER

Laser Field -Assisted Spin Tunnelling Through Quantum Dot System

Salah A. H. Al Murshidee [1,2] *, *Ahmed Fadhil Almurshedi* [1]

[1] *Department of Physics, College of Science, Al Muthanna University, Al Muthanna,66001, Iraq*

[2] *College of Engineering, Al-Ayen University, Thi-Qar, Iraq*

ARTICLE INFO

Article History:
Received 03 September 2025
Accepted 20 December 2025
Published 01 January 2026

Keywords:
Nanoelectronics devices
Nanotechnology
Spintronic

ABSTRACT

An extended theoretical study to investigated the role of laser field in spintronic properties through quantum dot embedded between two normal leads is introduced. The Anderson model is used in our treatment to model the quantum dot energy level that hybridize with the leads to enable the spintronic tunneling process. An external magnetic field, the intra-dot Coulomb correlation on quantum dot and their coupling with the leads are incorporates in this study. The calculations declare that if the laser field is applied on quantum dot, a multiple transport channels are opened. Each spin energy level of quantum dot splits to three spin energy levels, resulting in the occurrence of the photon-assisted (FAT) peaks in total differential conductance spectrum. The positions of these peaks related to the peaks in differential conductance spectrum of the channels. An interesting result is the observation of photon-assisted (FAT) peak that can be generated in the Coulomb blockade effect around ($V_{Sb} = 0$) region, which is belong to one of the three opened channels in this region, depending on manipulating and tuning of the energy level of quantum dot and the external magnetic field. This peak clarifies that the linear behaviors of spin current and the device behave as resistor in this region. This feature can be utilized experimentally to estimate the behavior the spin current, differential conductance and their opened channels with spin bias variation, depending on the energy level of quantum and the external magnetic field measuring.

How to cite this article
Dehghankelishadi P, Dorkoosh FA. Pluronic based nano-delivery systems; Prospective warrior in war against cancer. J Nanostruct, 2026; 16(1):595-602. DOI: 10.22052/JNS.2026.01.053

INTRODUCTION

Quantum dot (QD) is fundamental structure of zero-dimensional system, where all electrons are confined in three directions, due to the confinement, the energy levels of quantum dot will be quantized and similar to the electronic levels of real atom which give rise to be named as artificial atoms [1,2]. Generally, the tunneling effects, quantum interference, and quantized energy levels can often have key roles in the charge and spin transport processes. The modern emerging field deals with the effective manipulation of the electron's charge and spin, this will have led to add a spin degree of freedom to the conventional charge-based technology, which has the prospective features of multi-functionality [3,4]. Study the electron and spin tunneling through quantum dot has attracted a lot

* *Corresponding Author Email: salah.almurshidee@mu.edu.iq*

of attention due to reveals new and unique effects such as Coulomb blockade effect, quantum Hall effect, Fano effect, Kondo effect, thermoelectric effect, and Photon-assisted tunneling effect (FAT), which makes the quantum dot a potential candidate as a building block for devices based on novel physics [1,5]. The (FAT), were electromagnetic (EM) field has interacted with the quantum dot system has received increased attention both experimentally and theoretically in recent year because of the potential application in quantum computing and photoelectron devices [6-8]. The physical mechanism of (FAT) effects is detected in the induced photon-current in the quantum dot system which has been investigated theoretically in quantum dot [9]. Later, different theoretical methods were proposed, such as the time-dependent Schrodinger equation, the transfer Hamiltonian method the Master equation, nonequilibrium Green function(NEGF) approach and the Keldysh nonequilibrium Green's function method. An important characteristic of these systems is that the electron in the system can exchange an energy with the external fields, leading to several new inelastic tunneling channels [7,10], resulting in an additional conductance peak with in the Coulomb blocked regime, this additional resonance is attributed to the (FAT) [11]. The manipulation of quantum dots embedded between two leads by a microwave and (EM) field is applied on quantum dot, a multiple transport channels are opened, which utilized for the possible to fabricate an important ingredient application of quantum dots as solid state quantum bits, single-photon transistors, spin filter, heat engine, quantum-dot thermospin, refrigerators, quantum computing and photoelectron devices [7,12-15].

In this work, we will present an extended theoretical study for the role of laser field in spintronic properties through quantum dot embedded between two normal leads. The nonequilibrium Green's function is used in this treatment to model the quantum dot energy level that hybridize with the leads to enable the spintronic tunneling process. An external magnetic field, the intra-dot Coulomb correlation on quantum dot and their coupling with the leads are incorporates. The occupation number on quantum dot is formulated and solved self-consistently, then it is used to derive the spin current tunneling through the system. The spin current shows three classified multiple spin currents channels due to split energy level of quantum dot to three multiple energy levels. These classified multiple spin currents channels are employed to investigate the spin tunneling properties and give us a chance to study and investigate many spin depending physical feature concerned to future spintronic applications especially in quantum computing.

THE MATHEMATICAL MODEL

The single impurity Anderson model is utilized to model the role of laser filed on system consist of single quantum (QD) embedded between normal leads, and assume that there is only two spin-split level of quantum dot duo to magnetic flux (Zeeman splitting), experience the photon mode of laser field incident directly on quantum dot. The Hamiltonian of the system considered in this can be written as the sum of three terms Eq.1 [7, 16,17].

The first term in Eq. 1 is the Hamiltonian for noninteracting electrons in the leads. Where $C_{k\alpha}^{\sigma+}$ ($C_{k\alpha}^{\sigma}$) is the creation (annihilation) operators of an electron with spin σ and energy $E_{k\alpha}^{\sigma}$ in the lead α(≡L,R). The second term in Eq. 1, is the Hamiltonian that describes the isolated quantum dot (QD), where $E_d^{\sigma}=E_d-\sigma H$, E_d, is the effective energy levels of the quantum dot (QD). where H denoted the Zeeman splitting energy. U represent the intra-quantum dot Coulomb correlation between spin up and spin down electrons on the (QD) and n_d^{σ} is the occupation number on the (QD) with spin σ where $n_d^{\sigma}=C^{\sigma+}(C^{\sigma})=(n_L^{\sigma}+n_R^{\alpha})/2$ and $C^{\sigma+}$ (C^{σ}) is the creation (annihilation) operator of a localized electron on the level E_d^{σ}. Where n_d^{σ} is the occupation number on the QD with spin σ due to the lead α and is given by Eq. 2 [18].

$$n_{\alpha}^{\sigma}=\sum_{n=0,\mp 1}K_n\int_{u_{0\alpha}}^{u_{\alpha}^{\sigma}}\rho_d^{\sigma}(E)f_{\alpha}^{\sigma}(E,T)dE \qquad (2)$$

$$H=\sum_{k_{\alpha},\sigma}E_{k_{\alpha}}C_{k_{\alpha}}^{\sigma+}C_{k_{\alpha}}^{\sigma}+\sum_{\sigma}E_d^{\sigma}n_d^{\sigma}+Un_d^{\sigma}n_d^{-\sigma}+\sum_{k\alpha,\sigma}(V_{k_{\alpha}}C_{k_{\alpha}}^{\sigma+}C_d^{\sigma}+V_{k_{\alpha}}^{*}C_d^{\sigma+}C_{k_{\alpha}}^{\sigma}) \qquad (1)$$

Where u_0^{α} is the band bottom of the leads α, μ_{α}^{σ} is the electrochemical potential on the lead αin the presence of spin bias. f_{α}^{σ} (E, T_{α}^{σ}) is the Fermi distribution function for the lead α and ρ_d^{σ} is the local density of states on the quantum dot (QD) which is coupled to the lead αand is given by Eq. 3 [7,19].

Where Γ_{α}^{σ} is the broadening in the energy levels of the QD due to the coupling with the lead α. Γ_L broadening due to laser field coupling interaction. The third term in Eq. 1 is the Hamiltonian that describes the quantum dot -leads interaction, where $V_{k\alpha}$ is the hybridization matrix elements between the quantum dot and the leadα.By using the Taylor expansion for Fermi distribution function around E=μ_{α} in the interval ($-k_BT_{\alpha} \leq \mu_{\alpha} \leq k_BT_{\alpha}$) we can solve Eq. 2 to calculate the occupation number on the QD with spinσ due to the lead α as Eq. 4.

The electrical current I^{σ}, flowing through the active region (QD) in the spin channel σ in the case of non-equilibrium due to applying spin bias, is given by the Eq. 5 [20,21].

By using Eqs. 2 and 3 in Eq. 4, one can write Eq. 4 in term of Eq. 2 as the following relation:

$$I^{\sigma} = \frac{e}{h}\frac{2\pi\Gamma_L^{\sigma}\Gamma_R^{\sigma}}{\Gamma_L^{\sigma}+\Gamma_R^{\sigma}}[n_L^{\sigma} - n_R^{\sigma}]$$

The spin current and differential conductance can be given by the following relations [21,22-24]:

$$I_S = \frac{\hbar}{2}(I^{\sigma} - I^{-\sigma}),\ D = \frac{\partial I}{\partial(eV_{Sb})}$$

RESULTS AND DISCUSSION

The role of laser field which is electromagnetic (EM) field on spin tunneling through the system of quantum dot between two normal leads well be investigated in case of weak coupling regime and the system is in thermal equilibrium at low

$$\rho_d^{\sigma}(E) = \frac{1}{\pi}\frac{\Gamma_{\alpha}^{\sigma}+2\Gamma_L}{(E-E_n^{\sigma})^2+(\Gamma_{\alpha}^{\sigma}+2\Gamma_L)^2} \tag{3}$$

Where $E_n^{\sigma} = E_d^{\sigma} + n\eta\omega$, and ω is the the harmonics frequency with (n = −1,0,1)

$$K_0 = \frac{\Gamma_{\alpha}^{\sigma}}{\Gamma_{\alpha}^{\sigma}+2\Gamma_L} \quad , \quad K_{-1} = K_1 = \frac{\Gamma_L}{\Gamma_{\alpha}^{\sigma}+2\Gamma_L}$$

$$\begin{aligned} n_{\alpha}^{\sigma} = \sum_{n=0,\pm1} K_n \Bigg\{ & -\tan^{-1}\left(\frac{u_{0\alpha} - (\mu_{\alpha}^{\sigma} - k_BT_{\alpha}) - E_d^{\sigma} + n\hbar\omega)}{\Gamma_{\alpha}^{\sigma}+2\Gamma_L}\right) + \left[1 - A_{0\alpha ij}^{\sigma} + A_{2\alpha ij}^{\sigma}(\Gamma_{\alpha}^{\sigma}+2\Gamma_L)^2\right]\tan^{-1}\left(\frac{\mu_{\alpha}^{\sigma} - k_BT_{\alpha} - E^{\sigma} + n\hbar\omega}{\Gamma_{\alpha}^{\sigma}+2\Gamma_L}\right) \\ & + \left[A_{0\alpha ij}^{\sigma} - A_{2\alpha ij}^{\sigma}(\Gamma_{\alpha}^{\sigma}+2\Gamma_L)^2\right]\tan^{-1}\left(\frac{\mu_{\alpha}^{\sigma} + k_BT_{\alpha} - E_d^{\sigma} + n\hbar\omega}{\Gamma_{\alpha}^{\sigma}+2\Gamma_L}\right) \\ & + \frac{1}{2}\left[A_{1\alpha ij}^{\sigma}\Gamma_{i\alpha}^{\sigma} - A_{3\alpha ij}^{\sigma}(\Gamma_{\alpha}^{\sigma}+2\Gamma_L)^3\right]\ln\frac{(\mu_{\alpha}^{\sigma} + k_BT_{\alpha}^{\sigma} - E_d^{\sigma} + n\hbar\omega)^2 + (\Gamma_{\alpha}^{\sigma}+2\Gamma_L)^2}{(\mu_{\alpha}^{\sigma} - k_BT_{\alpha}^{\sigma} - E_d^{\sigma} + n\hbar\omega)^2 + (\Gamma_{\alpha}^{\sigma}+2\Gamma_L)^2} + 4A_3(\Gamma_{\alpha}^{\sigma}+2\Gamma_L)(E_d^{\sigma} + n\hbar\omega \\ & - \mu_{\alpha}^{\sigma})k_BT_{\alpha}^{\sigma} \quad \Bigg\} \end{aligned} \tag{4}$$

where

$$\begin{aligned} A_{0\alpha ij}^{\sigma} &= a_0 + a_1(E_d^{\sigma} + n\hbar\omega - \mu_{\alpha}^{\sigma}) + a_3(E_d^{\sigma} + n\hbar\omega - \mu_{\alpha}^{\sigma})^3 \\ A_{1\alpha ij}^{\sigma} &= a_1 + 3a_3(E_d^{\sigma} + n\hbar\omega - \mu_{\alpha}^{\sigma})^2 \\ A_{2\alpha ij}^{\sigma} &= 3a_3(E_d^{\sigma} + n\hbar\omega - \mu_{\alpha}^{\sigma}) \\ A_{3\alpha ij}^{\sigma} &= a_3 \end{aligned}$$

with $a_0 = 0.5$, $a_1 = -\frac{0.25}{k_BT_{\alpha}^{\sigma}}$, $a_3 = \frac{0.02083333}{(k_BT_{\alpha}^{\sigma})^3}$

$$I^{\sigma} = \frac{e}{h}\frac{2\pi\Gamma_L^{\sigma}\Gamma_R^{\sigma}}{\Gamma_L^{\sigma}+\Gamma_R^{\sigma}} \sum_{n=0,\pm1} K_n \int_{u_0}^{u_\alpha} \rho_d^{\sigma}(E)[f(E,T_L) - f(E,T_R)]dE \quad (5)$$

temperature. Two parameters of the laser field are incorporate in this study, which are frequency and intensity of the laser beam applied to quantum dot, the harmonics frequency$\omega$with (n=-1,0,1) will be added to the energy level of quantum dot which splits each energy level into three levels (i.e.E_0^{σ} and $E_{\pm1}^{\sigma}$), while the intensity of the laser field incorporates as a tunneling rate (broadening),due to laser field coupling interaction with the leads that affected the density of state of quantum dot energy levels. In order to investigate the spin tunneling properties through the system considered in this study, spin bias will be applied to the leads ,while the quantum dot energy level position will be controlled by gate voltage.The spin current and it channels as well as the differential conductance are calculated to investigate the spin tunneling properties, The red, green and blue solid line represent the spin current and the differential conductance through the channels E_n^{σ},while the black dashed line represents the taotal spin current and differential conductance passing through all channels. In Fig. 1, the spin current as a function spin bias spin for different values of Zeeman splitting at positive value of quantum dot energy level is presented. In the absence of Laser field, the spin current shows step-like behavior due to the Coulomb blockade effect around spin bias equal zero, the width of step increases as Zeeman splitting increases, see Fig. 1(a and b) thick black line. When laser field presented, the quantum dot energy level E_d^{σ} will be splitting to three energy channels (i.e.E_0^{σ} and $E_{\pm1}^{\sigma}$). At the absence of Zeeman splitting the spin current of the energy channels E_0^{σ} and E_{-1}^{σ} show step-like behaviors,see Fig. 1a red and green solid line, while its linear in the region around spin bias equal zero through the energy channel $E_{\pm1}^{\sigma}$ and the device behaves as resistor, see Fig. 1a blue solid line. When the value of Zeeman splitting increases to 0.2 eV, the spin current of the energy channels E_0^{σ} and E_{+1}^{σ} show step-like behaviors as shown in Fig. 1b red and blue solid line, while its linear in the region around spin bias equal zero through the energy channel E_{-1}^{σ} and the device behaves as resistor see Fig. 1b green solid line. So that the total spin current behavior is enhanced due to tunneling through the energy channels $E_{\pm1}^{\sigma}$, see Figs. 1a and b black dashed line. But no obvious rule of the channel E_d^{σ} can be observed. Our study results show that the total spin current is increases as the laser field presented and the Photon-assisted tunneling appear. Fig. 1c and d, clarify the differential conductance as a function of spin bias. Fig. 1c black solid line, shows the differential conductance in the case of absence the laser field and Zeeman splitting equal zero, which exhibits two splitting peaks for certain spin bias polarity. The peaks are located on spin bias polarity equal to E_d+U, one con utilize in such experiments to determine the Coulomb correlation on quantum dot. When the Zeeman splitting increases to 0.2 eV, the differential conductance becomes relatively higher and the peaks become more separated, the peaks are lying at spin bias equal to Zeeman splitting, one can experimentally deduce the Zeeman splitting depending on the measured differential conductance, see the black solid line in Fig.1d. The red, green and blue lines, represent the differential conductance of the energy channels E_0^{σ} and $E_{\pm1}^{\sigma}$. In the presence of laser field and Zeeman splitting equal to zero, the laser field induce a peak emerge in the differential gab region around spin bias equal zero due to the spin tunneling current through the channel E_{+1}^{σ} in the Coulomb blockade regionsee see Fig. 1c blue solid line, further two peaks appear in the negative and positive spin bias regions represent the spin tunneling through the energy channel E_{-1}^{σ},these two peaks are located at spin bias polarity equal to $2E_{+1}^{\sigma}$, see Fig. 1c green solid line. one can experimentally deduce the energy level of quantum dot depending on the measured differential conductance. Our study results show that the laser field enhanced the total differential conductance, the peaks that appear in the total differential conductance are belong to the enrgy channels. One can experimentally deduce the behavior of the total differential conductance from the behavior of channels of differential conductance. As the Zeeman splitting increases to 0.2 eV, the feature of differential conductance of the energy channels E_{+1}^{σ} becomes relatively lesser and shows two peaks for certain spin bias polarity located at spin bias polarity equal to the

Zeeman splitting, see Fig. 1d blue solid line, while the differential conductance of the energy channel E_{-1}^{σ} exhibits three peaks, one of these peaks emerges in the differential gab region around spin bias equal zero due to the spin tunneling current through the channel E_{-1}^{σ} in the Coulomb blockade region (spin bias equal zero), the other two peaks are laying at the spin bias polarity equal to the energy $2E_{+1}^{\sigma}$ + H, see Fig. 1d green solid line, So that the Zeeman splitting induced more peaks in the total differential conductance, these peaks reflects exactly the peaks of the channels $E_{\pm1}^{\sigma}$, see dashed black line in Fig. 1c and d. From the results above , one can deduce the behavior of total differential conductance from the differential conductance of the energy channels $E_{\pm1}^{\sigma}$, also one can control the channel induce peak in the differential gab region around spin bias polarity , depending on the measured quantum dot energy level and Zeeman splitting.

In order to report physical nots about the position of quantum dot energy levels, all the above mentioned calculation are also achieved for negative value of quantum dot energy levels. In the case of presence laser field and absence of Zeeman splitting, the spin current relation through the energy channels E_{0}^{σ} and E_{+1}^{σ} show step-like behaviors see Fig. 2a red and blue solid lines, while its linear in the region around spin bias equal to zero through the channel E_{-1}^{σ} and the device behaves as resistor see Fig. 2a green solid line, while the laser field induces a peak emerge in the differential gab region around spin bias equal zero due to the spin tunneling current through the energy channe E_{-1}^{σ} l in the Coulomb blockade region, see Fig. 2c green line, further two peaks appear in the negative and positive spin bias regions represent the spin tunneling through

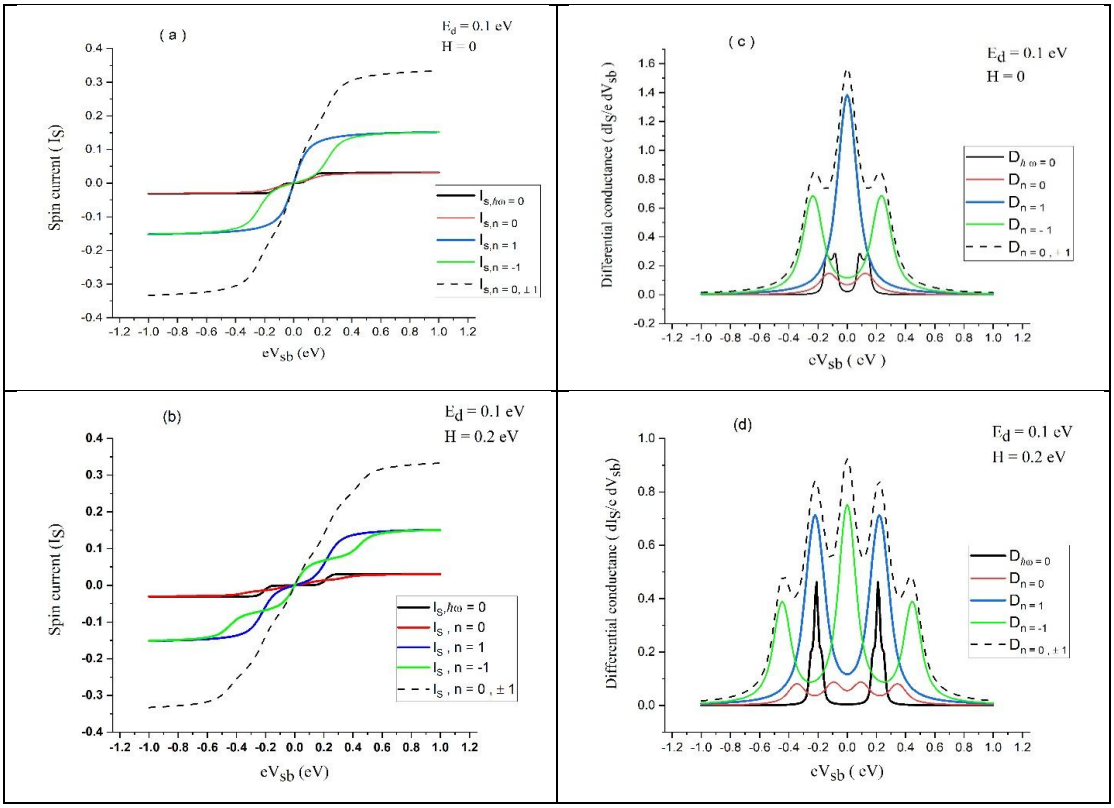

Fig. 1. (a) and (b)The spin current as a function of spin bias for different values of Zeeman splitting in the case of absence and presence of laser field. (c) and (d) the spin differential conductance as a function of spin bias for different values of Zeeman splitting in the case of absence and presence of laser field. The red, green and blue solid line represent the spin current and the differential conductance through the channels E_d^{σ}, E_d^{σ} -$\hbar\omega$ and E_d^{σ} + $\hbar\omega$ where (n=0,-1,+1), respectfully, while the black dashed line represents the taotal spin current and differential conductance passing through all channels. Other parameters are E_d=0.1eV, T_L=T_R=100K, Γ_{α}^{σ}=Γ_L=0.01eV, U=0.05eV, $\hbar\omega$=0.1eV.

the channel E_{+1}^{σ}, see Fig. 2c blue solid line. By comparing Fig. 1 with Fig. 2 in the case of absence Zeeman splitting, one can control experimentally which channel induces the current and the peak of differential conductance spectrum in the Coulomb blockade region, also one can deduce the behavior of quantum dots energy level with the spin bias variation depending on the measured differential conductance. When the Zeeman splitting increases to 0.2 eV, the spin current tunneling through all channels show step-like behaviors, no spin current induced in the region around spin bias equal to zero and the Coulomb blockade appear see Fig. 2b red , blue and green lines, the most important physical features are that the spin current through the two channels $E_{\pm1}^{\sigma}$ have same value and behavior which mean that the spin current through these channels are coherent current. The differential conductance spectrum shows corresponding splitting peaks for each spin polarity belong to the energy channels $E_{\pm1}^{\sigma}$ see Fig. 2d blue and green lines, these peaks reflected the splitting peaks in the total differential conductance spectrum see Fig. 2d black dashed line.

In order to report physical nots about the position of quantum dot energy levels, we now pay some attention to effect of tuning energy level of quantum on spin tunneling properties . In Fig. 3a and b, we plot the spin current as a function of quantum dot energy level in the absence and presence of laser field for different values of Zeeman splitting. When the value of Zeeman splitting is zero, the laser field induces two peaks in the spin current spectrum, one peak in the negative values of quantum dot energy level due to the tunneling through the energy

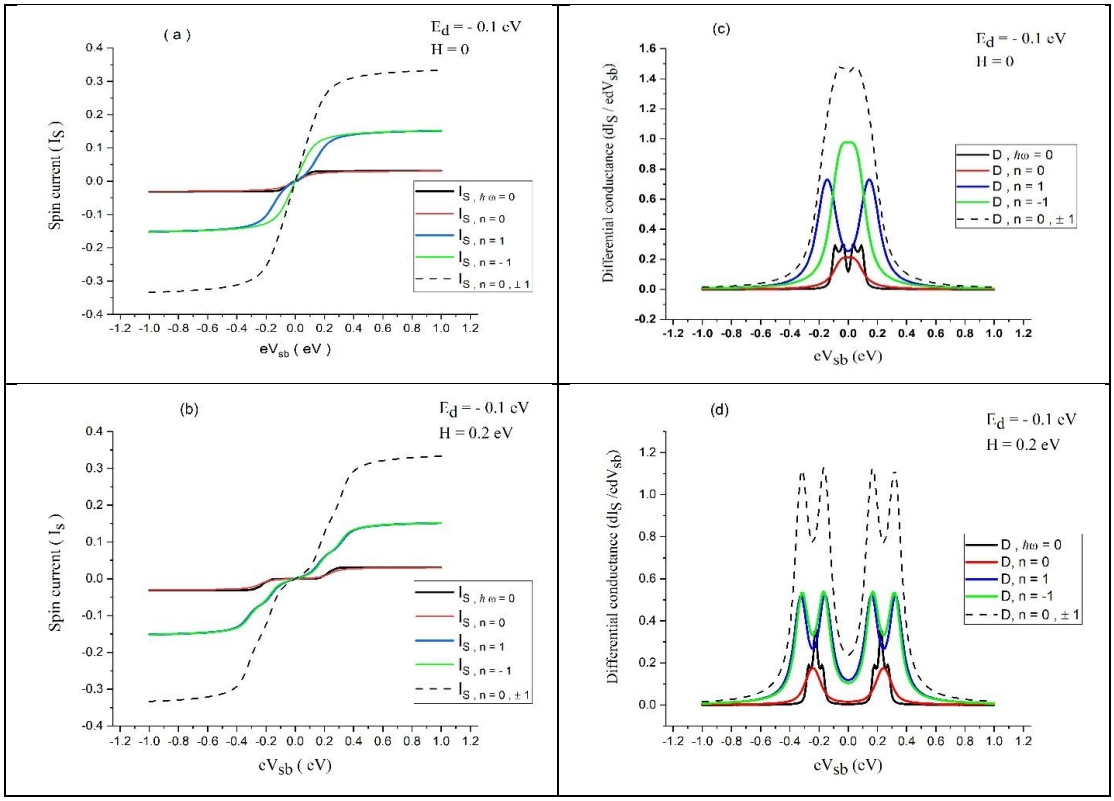

Fig. 2. (a) and (b)The spin current as a function of spin bias for different values of Zeeman splitting in the case of absence and presence of laser field. (c) and (d) The spin differential conductance as a function of spin bias for different values of Zeeman splitting in the case of absence and presence of laser field. The red, green and blue solid line represent the spin current and the differential conductance through the channels E_d^{σ}, E_d^{σ} -$\hbar\omega$ and E_d^{σ} + $\hbar\omega$ where (n=0,-1,+1), respectfully, while the black dashed line represents the taotal spin current and differential conductance passing through all channels. Other parameters are E_d=0.1eV, T_L=T_R=100K, Γ_{α}^{σ}=Γ_L=0.01eV, U=0.05eV, $\hbar\omega$=0.1eV.

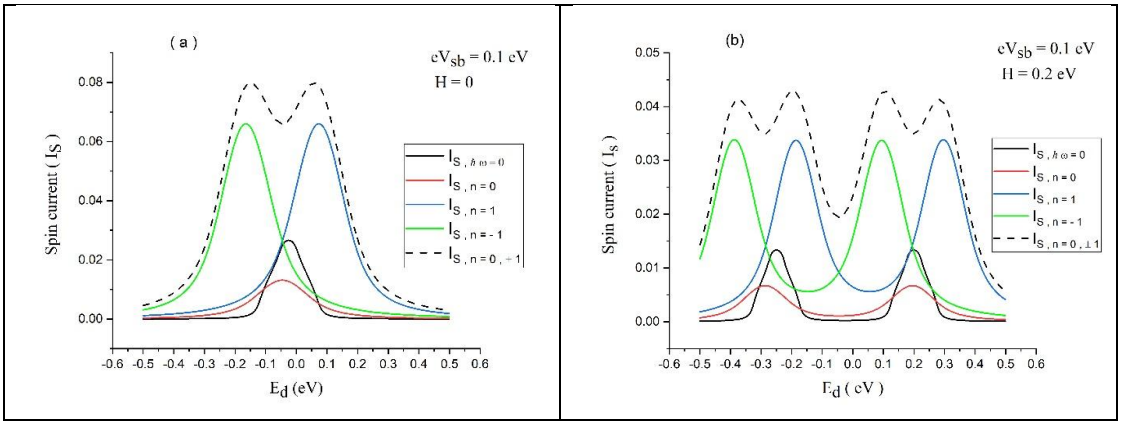

Fig. 3. (a) and (b)The spin current as a function of energy level of quantum dot for different values of Zeeman splitting in the case of absence and presence of laser field. Other parameters are eV_{sb}=0.1eV, T_L=T_R=100K, Γ_α^σ=Γ_L=0.01eV, U=0.05eV, $\hbar\omega$=0.1eV.

channel E_{-1}^{σ}, which is located at the quantum dot energy level equal to -2eV, the second peak in the positive values of quantum energy level due to the tunneling through the channel E_{+1}^{σ}, which is located at the quantum dot energy level equal to 0.1 eV,see Fig. 3a green and blue solid lines, these features confirm our results in Figs. 1 and 2, in the case of absence Zeeman splitting. As the value of Zeeman splitting increases to 0.2 eV, the laser field induces four peaks in the spin current spectrum, two peaks in the negative values of quantum dot energy level due to the tunneling through the channels $E_{\pm1}^{\sigma}$ located at the quantum dot energy level equal to-2 eV, and -4 eV, respectively, the second two peaks in the positive values of quantum dot energy level due to the tunneling through the channel $E_{\pm1}^{\sigma}$, which is located at the quantum dot energy level equal to 0.1 eV and 3 eV, see Fig.3b green and blue solid lines, these features confirm our results in Figs. 1 and 2.

CONCLUSION

The quantum dot system is very often directly serve as manipulating and controlling devices. They motivate us to investigate the spin tunneling properties in accurately controlled conditions. So the results discussed in our study are very important for future spintronic applications especially Photon- based spin electronics and quantum computing devices. The role of laser field in spintronic properties through quantum dot embedded between two normal leads is formulated based on the nonequilibrium Green's function model. An external magnetic field, the intra-dot Coulomb correlation on quantum dot and their coupling with the leads are incorporates in this study. The occupation number on quantum dot is solved self-consistently, then it is utilized to formulate the spin current tunneling through the system. The spin current and spin differential conductance shows three classified multiple channels due to split energy level of quantum dot to three multiple energy levels. These classified multiple channels are enhanced and induced the photon-assisted (FAT) peaks in total differential conductance spectrum. The positions of these peaks related to the peaks in differential conductance spectrum of the channels**.** An interesting results is the observation of photon-assisted (FAT) peak that can be generated in the Coulomb blockade effect region around spin bias equal zero, which is belong to one of the three opened channels in this region, which can be accurately determined by manipulating and tuning of the energy level of quantum dot and the external magnetic field. This peak clarifies that the resistor behaviors of spin current in this region. This results can be utilized experimentally to estimate the behavior the spin current, differential conductance from the behavior of the opened channels with spin bias variation, depending on the energy level of quantum and the external magnetic field measuring and vice versa.

CONFLICT OF INTEREST

The authors declare that there is no conflict of interests regarding the publication of this manuscript.

REFERENCES

1. He Z, Bai J, Li L, Zhi Q, Sun W. Photon-Assisted Electronic Transport Through an Asymmetrically Coupled Triple-Quantum Dot Interferometer. Moscow University Physics Bulletin. 2018;73(5):486-492.
2. Hanson R, Awschalom DD. Coherent manipulation of single spins in semiconductors. Nature. 2008;453(7198):1043-1049.
3. Tagani MB, Soleimani HR. Phonon-dependent transport through a serially coupled double quantum dot system. Chinese Physics B. 2014;23(5):057302.
4. Nattiq MA, Al-Mukh JM, Khalaf Al-zyadi JM. Spin polarization rate calculation for T-shaped double quantum dots coupled to (C- terminated ScC(1 1 1) surface) leads. J Magn Magn Mater. 2021;538:168284.
5. Likharev KK. Single-electron devices and their applications. Proc IEEE. 1999;87(4):606-632.
6. Meyer C, Elzerman JM, Kouwenhoven LP. Photon-Assisted Tunneling in a Carbon Nanotube Quantum Dot. Nano Lett. 2007;7(2):295-299.
7. Yang XF, Liu YS. A photon-assisted single-spin quantum-dot heat engine. Superlattices Microstruct. 2014;75:334-339.
8. Fernández-Fernández D, Picó-Cortés J, Vela Liñán S, Platero G. Photo-assisted spin transport in double quantum dots with spin–orbit interaction. Journal of Physics: Materials. 2023;6(3):034004.
9. Blick RH, Haug RJ, von Klitzing K, Eberl K. Photon-assisted tunneling through a double quantum dot. Surface Science. 1996;361-362:595-599.
10. Tang H-Z, An X-T, Wang A-K, Liu J-J. Photon assisted tunneling through three quantum dots with spin-orbit-coupling. J Appl Phys. 2014;116(6).
11. Blick RH, Haug RJ, van der Weide DW, von Klitzing K, Eberl K. Photon-assisted tunneling through a quantum dot at high microwave frequencies. Appl Phys Lett. 1995;67(26):3924-3926.
12. Wang Y, Huang C, Liao T, Chen J. Magnon-driven quantum dot refrigerators. Phys Lett A. 2015;379(47-48):3054-3058.
13. Shang R, Li H-O, Cao G, Xiao M, Tu T, Jiang H, et al. Photon-assisted-tunneling in a coupled double quantum dot under high microwave excitation powers. Appl Phys Lett. 2013;103(16).
14. Javadi A, Ding D, Appel MH, Mahmoodian S, Löbl MC, Söllner I, et al. Spin–photon interface and spin-controlled photon switching in a nanobeam waveguide. Nature Nanotechnology. 2018;13(5):398-403.
15. Pisani F, Gacemi D, Vasanelli A, Li L, Davies AG, Linfield E, et al. Electronic transport driven by collective light-matter coupled states in a quantum device. Nature Communications. 2023;14(1).
16. Li Z-Z, Leijnse M. Quantum interference in transport through almost symmetric double quantum dots. Physical Review B. 2019;99(12).
17. Weymann I, Wójcik KP, Majek P. Majorana-Kondo interplay in T-shaped double quantum dots. Physical Review B. 2020;101(23).
18. Al Murshidee SAH, Mohamad HK, Al-Mukh JM. Spin Transport Through Asymmetric Coupled Quantum Dots Between Ferromagnetic Leads. J Low Temp Phys. 2024;217(3-4):549-560.
19. Gadzuk JW. Surface molecules and chemisorption. Surface Science. 1974;43(1):44-60.
20. Yang F-B. Spin dependent Fano interference in a serial double quantum dot coupled to two topological superconducting quantum wires. Phys Lett A. 2021;401:127350.
21. Xu L, Li Z-J, Niu P, Nie Y-H. Nonequilibrium spin-polarized thermal transport in ferromagnetic–quantum dot–metal system. Phys Lett A. 2016;380(42):3553-3558.
22. Tasai T, Eto M. Effects of Polaron Formation in Semiconductor Quantum Dots on Transport Properties. J Phys Soc Jpn. 2003;72(6):1495-1500.
23. Thygesen KS, Jacobsen KW. Conduction Mechanism in a Molecular Hydrogen Contact. Phys Rev Lett. 2005;94(3).
24. Gong W, Xie X, Wei G. Coulomb-modified equilibrium and nonequilibrium properties in a double quantum dot Aharonov–Bohm–Fano interference device. J Appl Phys. 2010;107(7).